Corner stress singularities in a high-order plate theory

C.S. Huang *

Department of Civil Engineering, National Chiao, Tung University, 1001 Ta-Hsueh Road, Hsinchu 30050, Taiwan

Abstract

In the context of Lo's high-order plate theory, the present work applies the eigenfunction expansion approach to investigating the Williams-type stress singularities at the vertex of a wedge. The characteristic equations for determining the orders of singularities in stress resultants are separately developed for plates under extension and bending. The characteristic equations of plates under extension differ from those in generalized plane stress cases when the clamped boundary condition is imposed along one of the radial edges around the vertex. For plates under bending, the presented characteristic equations are identical to those of first-order shear deformation plate theory (FSDPT) if the clamping is not involved in boundary conditions along the radial edges of the vertex. The orders of singularities in stress resultants, which vary with the vertex angle, are plotted for various types of boundary conditions. The results are also comprehensively compared with those obtained according to other plate theories such as classical plate theory, FSDPT and Reddy's refined plate theory.

1. Introduction

Plates are widely used components in engineering applications in civil engineering, mechanical engineering, and aerospace engineering. The plate problem is a three-dimensional problem, but several plate theories have been proposed to simplify the three-dimensional problem into a two-dimensional one. Various plate theories were thoroughly reviewed in [1]. Re-entrant corners, at which stress singularities exist, are often encountered in analyses of plate problems. Although stress singularities are not of the real world, the exact nature of the singularities must be considered in a numerical solution to obtain an accurate and effective solution [2,3]. For example, Leissa et al. [4,5] analyzed free vibrations of circular sectorial plates with re-entrant corners or V-notches using the Ritz method, by intro-

ducing the so-called corner functions into the admissible functions to describe accurately the singular behaviors of thin plates. In the finite element approach, singular elements [6,7] are conventionally used to solve the problems with stress singularities by describing the exact order of stress singularities.

Many papers have addressed stress singularities at sharp corners in planar and three-dimensional elasticity theories (i.e., [8–12]), but only a few have considered corner stress singularities in various plate theories. According to the classical thin plate theory (CPT), Williams and his co-workers [13–15] first used the eigenfunction expansion approach to comprehensively investigate the corner stress singularities induced by homogeneous boundary conditions around a corner for isotropic plates and orthotropic plates. Rao [16] also applied the eigenfunction expansion technique to identify stress singularities at the interface corners of bi-material thin plates. Huang et al. [17] studied corner stress singularities for a sector plate with simply supported radial edges by finding the closed-form solution

---
* Tel.: +886-3-5712121x54962; fax: +886-3-5716257.
  E-mail address: cshuang@mail.nctu.edu.tw (C.S. Huang).

for the vibration of such a plate. Sinclair [18] elucidated the occurrence of logarithmic stress singularities in angular thin plates. Using the classical lamination theory, Ojikutu et al. [19] applied a finite difference scheme to determine the orders of stress singularities in a composite wedge.

It is well known that shear deformation and rotary inertial effects have to be considered for a moderately thick plate. Within the context of first-order shear deformation plate theory (FSDPT), Burton and Sinclair [20] first examined the Williams-type corner stress singularities by introducing a stress potential. Huang et al. [21] elucidated corner stress singularities in the closed-form solution for the vibration of a sector plate with simply supported radial edges. The results of Huang et al. [21] indicate the incompleteness of the solution of Burton and Sinclair [20], whose solution did not include singularities of shear forces. Recently, Huang [22] reinvestigated corner stress singularities by adopting Xie and Chaudhuri's approach [12] to solve the equilibrium equations in terms of displacement components, and obtained the orders of moment and shear force singularities identical to those obtained by Huang et al. [21] for the case of a corner with simply supported boundary conditions.

Although first-order shear deformation plate theory has been frequently applied to analyze thick plate problems, FSDPT has some limitations: the transverse shear strains are assumed to be constant through the thickness of the plate and a shear correction coefficient is needed. Some high-order plate theories (HPT) have been offered [1]. However, up to now, only one paper has considered the corner stress singularities in HPT. Huang [23] investigated the corner stress singularities by applying Reddy's refined plate theory [24], neglecting in-plane displacement of the mid-plane; and revealed that different plate theories (CPT, FSDPT and Reddy's plate theory) yields very different orders of stress singularities at a corner, under a fixed set of boundary conditions. Notably, Reddy's refined plate theory is equivalent to the high-order plate theories proposed by Schmidt [25] and Krishna Murty [26].

There are other high-order plate theories that are not equivalent to Reddy's. Bert [27] critically evaluated of various plate theories for nonlinear bending stress distribution and concluded that the plate theory of Lo et al. [28] offered a very accurate prediction. Furthermore, this high-order plate theory has also been used to study various types of plate problems (i.e., [29–31]). This theory differs from CPT, FSDPT and Reddy's plate theory not only in the assumed displacement fields, but also in the relations between strains and stresses. Unlike the generalized plane stress assumption of zero normal stress in the thickness direction used in CPT, FSDPT and Reddy's plate theory, Lo's theory uses the three-dimensional Hooke's law.

The aim of this work is to derive the characteristic equations to determine the orders of Williams-type stress singularities under various boundary conditions around a corner, by applying Lo's high-order plate theory. The characteristic equations are derived by adopting the approach of Hartranft and Sih [9] for three-dimensional elasticity problems. This paper investigates not only the singular behaviors of moments and shear forces but also the singular behaviors of in-plane forces. Notably, the singular behaviors of in-plane forces in FSDPT and Reddy's plate theory are the same as those for plane stress theory, so they were not discussed in [22,23]. The variations of the orders of singularities in stress resultants with the vertex angle of a wedge are graphically represented for different boundary conditions around the vertex. The current results are also comprehensively compared with those for CPT, FSDPT and Reddy's refined plate theory. The obtained singular behaviors may be used when sharp corners are involved to solve free vibration, static deflection, stress intensity and buckling problems for thick plates if Lo's high-order plate theory is applied.

2. Governing equations

As in Lo et al. [28] for Cartesian coordinates, the displacement field for a sector plate (or a wedge) with cylindrical coordinates as shown in Fig. 1 is given as

$$\bar{u}(r,\theta,z) = u(r,\theta) + z\psi_r(r,\theta) + z^2\xi_r(r,\theta) + z^3\phi_r(r,\theta),$$
(1a)

$$\bar{v}(r,\theta,z) = v(r,\theta) + z\psi_\theta(r,\theta) + z^2\xi_\theta(r,\theta) + z^3\phi_\theta(r,\theta),$$
(1b)

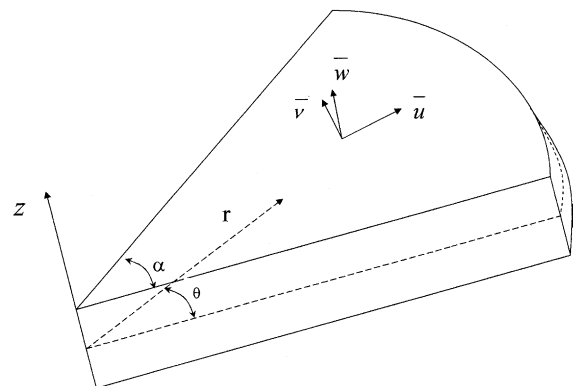$$\bar{w}(r,\theta,z) = w(r,\theta) + z\psi_z(r,\theta) + z^2\xi_z(r,\theta),$$
(1c)

Fig. 1. Coordinate system and positive displacement components for a wedge.

where $\bar{u}, \bar{v}$, and $\bar{w}$ are the displacement components in the r, θ, and z directions, respectively. This displacement field includes both in-plane and out-of-plane modes of deformation. There are 11 r and θ dependent displacement functions, namely, $u, v, w, \psi_r, \psi_\theta, \psi_z, \xi_r, \xi_\theta, \xi_z, \phi_r$, and ϕ_θ.

The principle of stationary potential energy is used to derive equilibrium equations through a variational approach. Without assuming generalized plane stress (i.e., $\sigma_{zz} = 0$), the three-dimensional Hooke's law for isotropic material is used. Eleven equilibrium equations for the 11 displacement functions can be found as follows, without external loading:

$$N_{r,r} + N_{r\theta,\theta}/r + (N_r - N_\theta)/r = 0, \tag{2}$$

$$N_{r\theta,r} + N_{\theta,\theta}/r + 2N_{r\theta}/r = 0, \tag{3}$$

$$Q_{r,r} + Q_{\theta,\theta}/r + Q_r/r = 0, \tag{4}$$

$$M_{r,r} + M_{r\theta,\theta}/r + (M_r - M_\theta)/r - Q_r = 0, \tag{5}$$

$$M_{r\theta,r} + M_{\theta,\theta}/r + 2M_{r\theta}/r - Q_\theta = 0, \tag{6}$$

$$R_{r,r} + R_{\theta,\theta}/r + R_r/r - N_z = 0, \tag{7}$$

$$P_{r,r} + P_{r\theta,\theta}/r + (P_r - P_\theta)/r - 2R_r = 0, \tag{8}$$

$$P_{r\theta,r} + P_{\theta,\theta}/r + 2P_{r\theta}/r - 2R_\theta = 0, \tag{9}$$

$$S_{r,r} + S_{\theta,\theta}/r + S_r/r - 2M_z = 0, \tag{10}$$

$$\overline{M}_{r,r} + \overline{M}_{r\theta,\theta}/r + (\overline{M}_r - \overline{M}_\theta)/r - 3S_r = 0, \tag{11}$$

$$\overline{M}_{r\theta,r} + \overline{M}_{\theta,\theta}/r + 2\overline{M}_{r\theta}/r - 3S_\theta = 0, \tag{12}$$

where the subscript, "α," denotes a partial differential with respect to the independent variable α. In addition, 11 boundary conditions for the r- and θ-constant edges can also be derived. Along a radial edge, one member of each of the following 11 products must be prescribed: $uN_{r\theta}, vN_\theta, wQ_\theta, \psi_r M_{r\theta}, \psi_\theta M_\theta, \psi_z R_\theta, \xi_r P_{r\theta}, \xi_\theta P_\theta, \xi_z S_\theta, \phi_r \overline{M}_{r\theta}$, and $\phi_\theta \overline{M}_\theta$. For the r-constant edge, one member of each of the following 11 products must also be prescribed: $uN_r, vN_{r\theta}, wQ_r, \psi_r M_r, \psi_\theta M_{r\theta}, \psi_z R_r, \xi_r P_r, \xi_\theta P_{r\theta}, \xi_z S_r, \phi_r \overline{M}_r$, and $\phi_\theta \overline{M}_{r\theta}$. Notably, the governing equations can also be obtained by multiplying the well-known three-dimensional equilibrium equations in continuum mechanics with 1, z, z^2, or z^3, and integrating them with respect to z. To the author's knowledge, these equilibrium equations (Eqs. (2)–(12)) have not been shown before.

The resultant forces in Eqs. (2)–(12) are defined as follows:

$$\begin{bmatrix} N_r & N_\theta & N_z & N_{r\theta} & Q_r & Q_\theta \\ M_r & M_\theta & M_z & M_{r\theta} & R_r & R_\theta \end{bmatrix}$$
$$= \int_{-h/2}^{h/2} \begin{Bmatrix} 1 \\ z \end{Bmatrix} (\sigma_{rr} \quad \sigma_{\theta\theta} \quad \sigma_{zz} \quad \sigma_{r\theta} \quad \sigma_{rz} \quad \sigma_{\theta z})\,\mathrm{d}z, \tag{13a}$$

$$\begin{bmatrix} P_r & P_\theta & P_{r\theta} \\ \overline{M}_r & \overline{M}_\theta & \overline{M}_{r\theta} \end{bmatrix} = \int_{-h/2}^{h/2} \begin{Bmatrix} z^2 \\ z^3 \end{Bmatrix} (\sigma_{rr} \quad \sigma_{\theta\theta} \quad \sigma_{r\theta})\,\mathrm{d}z, \tag{13b}$$

$$(S_r \quad S_\theta) = \int_{-h/2}^{h/2} z^2 (\sigma_{rz} \quad \sigma_{\theta z})\,\mathrm{d}z, \tag{13c}$$

where σ_{ij} are stress components. From Eqs. (13a–c) and using the three-dimensional Hooke's law for isotropic material and strain–displacement relations for infinitesimal deformation, we can obtain the following relations between the resultant forces and the displacement functions:

$$N_r = h[(\lambda + 2G)u_{,r} + \lambda(u + v_{,\theta})/r + \lambda\psi_z] \\ + \frac{h^3}{12}[(\lambda + 2G)\xi_{r,r} + \lambda(\xi_r + \xi_{\theta,\theta})/r], \tag{14a}$$

$$N_\theta = h[\lambda u_{,r} + (\lambda + 2G)(u + v_{,\theta})/r + \lambda\psi_z] \\ + \frac{h^3}{12}[\lambda\xi_{r,r} + (\lambda + 2G)(\xi_r + \xi_{\theta,\theta})/r], \tag{14b}$$

$$N_z = h[\lambda u_{,r} + \lambda(u + v_{,\theta})/r + (\lambda + 2G)\psi_z] \\ + \frac{h^3}{12}[\lambda\xi_{r,r} + \lambda(\xi_r + \xi_{\theta,\theta})/r], \tag{14c}$$

$$N_{r\theta} = Gh[v_{,r} - (v - u_{,\theta})/r] + \frac{Gh^3}{12}[\xi_{\theta,r} - (\xi_\theta - \xi_{r,\theta})/r], \tag{14d}$$

$$Q_r = Gh(\psi_r + w_{,r}) + \frac{Gh^3}{12}(3\phi_r + \xi_{z,r}), \tag{14e}$$

$$Q_\theta = Gh(\psi_\theta + w_{,\theta}/r) + \frac{Gh^3}{12}(3\phi_\theta + \xi_{z,\theta}/r), \tag{14f}$$

$$M_r = \frac{h^3}{12}[(\lambda + 2G)\psi_{r,r} + \lambda(\psi_r + \psi_{\theta,\theta})/r + 2\lambda\xi_z] \\ + \frac{h^5}{80}[(\lambda + 2G)\phi_{r,r} + \lambda(\phi_r + \phi_{\theta,\theta})/r], \tag{14g}$$

$$M_\theta = \frac{h^3}{12}[\lambda\psi_{r,r} + (\lambda + 2G)(\psi_r + \psi_{\theta,\theta})/r + 2\lambda\xi_z] \\ + \frac{h^5}{80}[\lambda\phi_{r,r} + (\lambda + 2G)(\phi_r + \phi_{\theta,\theta})/r], \tag{14h}$$

$$M_z = \frac{h^3}{12}[\lambda\psi_{r,r} + \lambda(\psi_r + \psi_{\theta,\theta})/r + 2(\lambda + 2G)\xi_z]$$
$$+ \frac{h^5}{80}[\lambda\phi_{r,r} + \lambda(\phi_r + \phi_{\theta,\theta})/r], \tag{14i}$$

$$M_{r\theta} = \frac{Gh^3}{12}[(\psi_{r,\theta} - \psi_\theta)/r + \psi_{\theta,r}]$$
$$+ \frac{Gh^5}{80}[(\phi_{r,\theta} - \phi_\theta)/r + \phi_{\theta,r}], \tag{14j}$$

$$R_r = \frac{Gh^3}{12}(2\xi_r + \psi_{z,r}), \tag{14k}$$

$$R_\theta = \frac{Gh^3}{12}(2\xi_\theta + \psi_{z,\theta}/r), \tag{14l}$$

$$P_r = \frac{h^3}{12}[(\lambda + 2G)u_{,r} + \lambda(u + v_{,\theta})/r + \lambda\psi_z]$$
$$+ \frac{h^5}{80}[(\lambda + 2G)\xi_{r,r} + \lambda(\xi_r + \xi_{\theta,\theta})/r], \tag{14m}$$

$$P_\theta = \frac{h^3}{12}[\lambda u_{,r} + (\lambda + 2G)(u + v_{,\theta})/r + \lambda\psi_z]$$
$$+ \frac{h^5}{80}[\lambda\xi_{r,r} + (\lambda + 2G)(\xi_r + \xi_{\theta,\theta})/r], \tag{14n}$$

$$P_{r\theta} = \frac{Gh^3}{12}[v_{,r} - (v - u_{,\theta})/r] + \frac{Gh^5}{80}[\xi_{\theta,r} - (\xi_\theta - \xi_{r,\theta})/r], \tag{14o}$$

$$\overline{M}_r = \frac{h^5}{80}[(\lambda + 2G)\psi_{r,r} + \lambda(\psi_r + \psi_{\theta,\theta})/r + 2\lambda\xi_z]$$
$$+ \frac{h^7}{448}[(\lambda + 2G)\phi_{r,r} + \lambda(\phi_r + \phi_{\theta,\theta})/r], \tag{14p}$$

$$\overline{M}_\theta = \frac{h^5}{80}[\lambda\psi_{r,r} + (\lambda + 2G)(\psi_r + \psi_{\theta,\theta})/r + 2\lambda\xi_z]$$
$$+ \frac{h^7}{448}[\lambda\phi_{r,r} + (\lambda + 2G)(\phi_r + \phi_{\theta,\theta})/r], \tag{14q}$$

$$\overline{M}_{r\theta} = \frac{Gh^5}{80}[(\psi_{r,\theta} - \psi_\theta)/r + \psi_{\theta,r}]$$
$$+ \frac{Gh^7}{448}[(\phi_{r,\theta} - \phi_\theta)/r + \phi_{\theta,r}], \tag{14r}$$

$$S_r = \frac{Gh^3}{12}(\psi_r + w_{,r}) + \frac{Gh^5}{80}(3\phi_r + \xi_{z,r}), \tag{14s}$$

$$S_\theta = \frac{Gh^3}{12}(\psi_\theta + w_{,\theta}/r) + \frac{Gh^5}{80}(3\phi_\theta + \xi_{z,\theta}/r), \tag{14t}$$

where G is the shear modulus, λ is one of the Lame's constants, and h is the thickness of the plate.

Substituting Eqs. (14a)–(14t) into Eqs. (2)–(12) with careful arrangement yields the equilibrium equations in terms of displacement functions:

$$u_{,rr} + \frac{u_{,r}}{r} - \frac{u}{r^2} + \frac{G}{(2G+\lambda)}\frac{u_{,\theta\theta}}{r^2} + \frac{G+\lambda}{2G+\lambda}\frac{v_{,r\theta}}{r} - \frac{3G+\lambda}{2G+\lambda}\frac{v_{,\theta}}{r^2}$$
$$+ \frac{\lambda}{2G+\lambda}\psi_{z,r} + \frac{h^2}{12}\left\{\xi_{r,rr} + \frac{\xi_{r,r}}{r} - \frac{\xi_r}{r^2} + \frac{G}{2G+\lambda}\frac{\xi_{r,\theta\theta}}{r^2}\right.$$
$$\left. + \frac{G+\lambda}{2G+\lambda}\frac{\xi_{\theta,r\theta}}{r} - \frac{3G+\lambda}{2G+\lambda}\frac{\xi_{\theta,\theta}}{r^2}\right\} = 0, \tag{15}$$

$$v_{,rr} + \frac{v_{,r}}{r} - \frac{v}{r^2} + \frac{2G+\lambda}{G}\frac{v_{,\theta\theta}}{r^2} + \frac{\lambda+G}{G}\frac{u_{,r\theta}}{r} + \frac{3G+\lambda}{G}\frac{u_{,\theta}}{r^2}$$
$$+ \frac{\lambda}{G}\frac{\psi_{z,\theta}}{r} + \frac{h^2}{12}\left\{\xi_{\theta,rr} + \frac{\xi_{\theta,r}}{r} - \frac{\xi_\theta}{r^2} + \frac{2G+\lambda}{G}\frac{\xi_{\theta,\theta\theta}}{r^2}\right.$$
$$\left. + \frac{\lambda+G}{G}\frac{\xi_{r,r\theta}}{r} + \frac{3G+\lambda}{G}\frac{\xi_{r,\theta}}{r^2}\right\} = 0, \tag{16}$$

$$w_{,rr} + \frac{w_{,r}}{r} + \frac{w_{,\theta\theta}}{r^2} + \psi_{r,r} + \frac{\psi_r}{r} + \frac{\psi_{\theta,\theta}}{r} + \frac{h^2}{12}\left\{\xi_{z,rr} + \frac{\xi_{z,r}}{r}\right.$$
$$\left. + \frac{\xi_{z,\theta\theta}}{r^2} + 3\left(\phi_{r,r} + \frac{\phi_r}{r} + \frac{\phi_{\theta,\theta}}{r}\right)\right\} = 0, \tag{17}$$

$$-\frac{12}{h^2}\frac{G}{2G+\lambda}(w_{,r} + \psi_r) + \psi_{r,rr} + \frac{\psi_{r,r}}{r} - \frac{\psi_r}{r^2} + \frac{G}{2G+\lambda}\frac{\psi_{r,\theta\theta}}{r^2}$$
$$+ \frac{G+\lambda}{2G+\lambda}\frac{\psi_{\theta,r\theta}}{r} - \frac{3G+\lambda}{2G+\lambda}\frac{\psi_{\theta,\theta}}{r^2} + \frac{-G+2\lambda}{2G+\lambda}\xi_{z,r}$$
$$- \frac{3G}{2G+\lambda}\phi_r + \frac{3h^2}{20}\left\{\phi_{r,rr} + \frac{\phi_{r,r}}{r} - \frac{\phi_r}{r^2} + \frac{G}{2G+\lambda}\frac{\phi_{r,\theta\theta}}{r^2}\right.$$
$$\left. + \frac{G+\lambda}{2G+\lambda}\frac{\phi_{\theta,r\theta}}{r} - \frac{3G+\lambda}{2G+\lambda}\frac{\phi_{\theta,\theta}}{r^2}\right\} = 0, \tag{18}$$

$$-\frac{12}{h^2}\left(\frac{w_{,\theta}}{r} + \psi_\theta\right) + \psi_{\theta,rr} + \frac{\psi_{\theta,r}}{r} - \frac{\psi_\theta}{r^2} + \frac{2G+\lambda}{G}\frac{\psi_{\theta,\theta\theta}}{r^2}$$
$$+ \frac{G+\lambda}{G}\frac{\psi_{r,r\theta}}{r} + \frac{3G+\lambda}{G}\frac{\psi_{r,\theta}}{r^2} + \frac{-G+2\lambda}{G}\frac{\xi_{z,\theta}}{r} - 3\phi_\theta$$
$$+ \frac{3h^2}{20}\left\{\phi_{\theta,rr} + \frac{\phi_{\theta,r}}{r} - \frac{\phi_\theta}{r^2} + \frac{2G+\lambda}{G}\frac{\phi_{\theta,\theta\theta}}{r^2} + \frac{G+\lambda}{G}\frac{\phi_{r,r\theta}}{r}\right.$$
$$\left. + \frac{3G+\lambda}{G}\frac{\phi_{r,\theta}}{r^2}\right\} = 0, \tag{19}$$

$$\frac{\lambda}{G}\left(u_{,r} + \frac{u}{r} + \frac{v_{,\theta}}{r}\right) + \frac{2G+\lambda}{G}\psi_z - \frac{h^2}{12}\left\{\psi_{z,rr} + \frac{\psi_{z,r}}{r} + \frac{\psi_{z,\theta\theta}}{r^2}\right.$$
$$\left. + \frac{2G-\lambda}{G}\left(\xi_{r,r} + \frac{\xi_r}{r} + \frac{\xi_{\theta,\theta}}{r}\right)\right\} = 0, \tag{20}$$

$$u_{,rr} + \frac{u_{,r}}{r} - \frac{u}{r^2} + \frac{G}{2G+\lambda} \frac{u_{,\theta\theta}}{r^2} + \frac{G+\lambda}{2G+\lambda} \frac{v_{,r\theta}}{r} - \frac{3G+\lambda}{2G+\lambda} \frac{v_{,\theta}}{r^2}$$

$$- \frac{2G-\lambda}{2G+\lambda} \psi_{z,r} - \frac{4G}{2G+\lambda} \xi_r + \frac{3h^2}{20} \left\{ \xi_{r,rr} + \frac{\xi_{r,r}}{r} - \frac{\xi_r}{r^2} \right.$$

$$\left. + \frac{G}{2G+\lambda} \frac{\xi_{r,\theta\theta}}{r^2} + \frac{G+\lambda}{2G+\lambda} \frac{\xi_{\theta,r\theta}}{r} - \frac{3G+\lambda}{2G+\lambda} \frac{\xi_{\theta,\theta}}{r^2} \right\} = 0,$$

$$(21)$$

$$v_{,rr} + \frac{v_{,r}}{r} - \frac{v}{r^2} + \frac{2G+\lambda}{G} \frac{v_{,\theta\theta}}{r^2} + \frac{G+\lambda}{G} \frac{u_{,r\theta}}{r} + \frac{3G+\lambda}{G} \frac{u_{,\theta}}{r^2}$$

$$+ \frac{-2G+\lambda}{G} \frac{\psi_{z,\theta}}{r} - 4\xi_\theta + \frac{3h^2}{20} \left\{ \xi_{\theta,rr} + \frac{\xi_{\theta,r}}{r} - \frac{\xi_\theta}{r^2} \right.$$

$$\left. + \frac{2G+\lambda}{G} \frac{\xi_{\theta,\theta\theta}}{r^2} + \frac{G+\lambda}{G} \frac{\xi_{r,r\theta}}{r} + \frac{3G+\lambda}{G} \frac{\xi_{r,\theta}}{r^2} \right\} = 0,$$

$$(22)$$

$$w_{,rr} + \frac{w_{,r}}{r} + \frac{w_{,\theta\theta}}{r^2} + \frac{G-2\lambda}{G} \left(\psi_{r,r} + \frac{\psi_r}{r} + \frac{\psi_{\theta,\theta}}{r} \right)$$

$$- \frac{4(2G+\lambda)}{G} \xi_z + \frac{3h^2}{20} \left\{ \xi_{z,rr} + \frac{\xi_{z,r}}{r} + \frac{\xi_{z,\theta\theta}}{r^2} \right.$$

$$\left. + \frac{3G-2\lambda}{G} \left(\phi_{r,r} + \frac{\phi_r}{r} + \frac{\phi_{\theta,\theta}}{r} \right) \right\} = 0,$$

$$(23)$$

$$- \frac{20G}{h^2(2G+\lambda)}(w_{,r} + \psi_r) + \psi_{r,rr} + \frac{\psi_{r,r}}{r} - \frac{\psi_r}{r^2} + \frac{G}{2G+\lambda} \frac{\psi_{r,\theta\theta}}{r^2}$$

$$+ \frac{G+\lambda}{2G+\lambda} \frac{\psi_{\theta,r\theta}}{r} - \frac{3G+\lambda}{2G+\lambda} \frac{\psi_{\theta,\theta}}{r^2} - \frac{3G-2\lambda}{2G+\lambda} \xi_{z,r}$$

$$- \frac{9G}{2G+\lambda} \phi_r + \frac{5h^2}{28} \left\{ \phi_{r,rr} + \frac{\phi_{r,r}}{r} - \frac{\phi_r}{r^2} + \frac{G}{2G+\lambda} \frac{\phi_{r,\theta\theta}}{r^2} \right.$$

$$\left. + \frac{G+\lambda}{2G+\lambda} \frac{\phi_{\theta,r\theta}}{r} - \frac{3G+\lambda}{2G+\lambda} \frac{\phi_{\theta,\theta}}{r^2} \right\} = 0,$$

$$(24)$$

$$- \frac{20}{h^2} \left(\frac{w_{,\theta}}{r} + \psi_\theta \right) + \psi_{\theta,rr} + \frac{\psi_{\theta,r}}{r} - \frac{\psi_\theta}{r^2} + \frac{2G+\lambda}{G} \frac{\psi_{\theta,\theta\theta}}{r^2}$$

$$+ \frac{G+\lambda}{G} \frac{\psi_{r,r\theta}}{r} + \frac{3G+\lambda}{G} \frac{\psi_{r,\theta}}{r^2} + \frac{-3G+2\lambda}{G} \frac{\xi_{z,\theta}}{r} - 9\phi_\theta$$

$$+ \frac{5h^2}{28} \left\{ \phi_{\theta,rr} + \frac{\phi_{\theta,r}}{r} - \frac{\phi_\theta}{r^2} + \frac{2G+\lambda}{G} \frac{\phi_{\theta,\theta\theta}}{r^2} + \frac{G+\lambda}{G} \frac{\phi_{r,r\theta}}{r} \right.$$

$$\left. + \frac{3G+\lambda}{G} \frac{\phi_{r,\theta}}{r^2} \right\} = 0,$$

$$(25)$$

The above equations were developed with the aid of the symbolic logic software program MATHMATICA.

Note that Eqs. (15)–(25) partially decouple such that the equations can be combined into two groups. One group comprises Eqs. (15), (16), (20), (21), and (22) for the displacement functions u, v, ψ_z, ξ_r, and ξ_θ, which are related to the extension of the middle plane of the plate. The second group consists of the other equations, which describe the behavior of a plate under bending. Consequently, in the following, we investigate the stress singularities for these two groups separately.

3. Stress singularities for plates under extension

Here, a plate under extension means that in-plane loading is applied to the plate and may cause the extension of the middle plane of the plate. Some of Eqs. (15), (16), (20), (21), and (22) can be further simplified through some mathematic manipulations. From Eqs. (15) and (21), we can obtain

$$\frac{2G}{2G+\lambda} \psi_{z,r} + \frac{4G}{2G+\lambda} \xi_r - \frac{h^2}{15} \left\{ \xi_{r,rr} + \frac{\xi_{r,r}}{r} - \frac{\xi_r}{r^2} \right.$$

$$\left. + \frac{G}{2G+\lambda} \frac{\xi_{r,\theta\theta}}{r^2} + \frac{G+\lambda}{2G+\lambda} \frac{\xi_{\theta,r\theta}}{r} - \frac{3G+\lambda}{2G+\lambda} \frac{\xi_{\theta,\theta}}{r^2} \right\} = 0.$$

$$(26)$$

From Eqs. (16) and (22), the following equation can be obtained

$$\frac{2}{r} \psi_{z,\theta} + 4\xi_\theta - \frac{h^2}{15} \left\{ \xi_{\theta,rr} + \frac{\xi_{\theta,r}}{r} - \frac{\xi_\theta}{r^2} + \frac{2G+\lambda}{G} \frac{\xi_{\theta,\theta\theta}}{r^2} \right.$$

$$\left. + \frac{\lambda+G}{G} \frac{\xi_{r,r\theta}}{r} + \frac{3G+\lambda}{G} \frac{\xi_{r,\theta}}{r^2} \right\} = 0.$$

$$(27)$$

Consequently, the stress singularities for plates under extension will be investigated by solving Eqs. (15), (16), (20), (26), and (27) and employing some combinations of boundary conditions along radial edges.

3.1. Construction of the series solution

An eigenfunction expansion approach similar to that used in [23] is applied to solve Eqs. (15), (16), (20), (26), and (27). Let

$$u = \sum_{m=0}^{\infty} \sum_{n=0,2}^{\infty} r^{\lambda_m+n} U_n^{(m)}(\theta, \lambda_m),$$

$$v = \sum_{m=0}^{\infty} \sum_{n=0,2}^{\infty} r^{\lambda_m+n} V_n^{(m)}(\theta, \lambda_m),$$

$$\xi_r = \sum_{m=0}^{\infty} \sum_{n=0,2}^{\infty} r^{\lambda_m+n} \Omega_{rn}^{(m)}(\theta, \lambda_m),$$

$$\xi_\theta = \sum_{m=0}^{\infty} \sum_{n=0,2}^{\infty} r^{\lambda_m+n} \Omega_{\theta n}^{(m)}(\theta, \lambda_m),$$

and

$$\psi_z = \sum_{m=0}^{\infty} \sum_{n=0,2}^{\infty} r^{\lambda_m+n+1} \Psi_{zn}^{(m)}(\theta, \lambda_m),$$

$$(28)$$

where the characteristic values λ_m are assumed to be constants and can be complex numbers. Notably, odd n in Eq. (28) will not give any additional solutions; therefore, they are excluded.

The regularity conditions at $r = 0$ require $\bar{u}, \bar{v}$, and $\bar{w}$ to be finite; therefore, the real part of λ_m has to exceed

zero. Consequently, the relations between stress resultants and displacement functions given in Eqs. (14a)–(14d) and (14k)–(14o) reveal that the solution given by Eq. (28) yields the singularities for N_r, N_θ, N_z, $N_{r\theta}$, P_r, P_θ, and $P_{r\theta}$ at $r = 0$ when the real part of λ_m is below one. Nevertheless, no singularities occur for the stress resultants R_r and R_θ.

Substituting Eq. (28) into Eqs. (15), (16), (20), (26), and (27) and requiring that the coefficients of r with different orders equal zero yield the following recurrent equations for $U_n^{(m)}$, $V_n^{(m)}$, $\Omega_{rn}^{(m)}$, $\Omega_{\theta n}^{(m)}$, and $\Psi_{zn}^{(m)}$:

$$\frac{h^2}{15}\left\{(\lambda_m + n + 3)(\lambda_m + n + 1)\Omega_{r(n+2)}^{(m)} + \frac{G}{2G+\lambda}\Omega_{r(n+2),\theta\theta}^{(m)}\right.$$
$$\left. + \frac{G+\lambda}{2G+\lambda}(\lambda_m + n + 2)\Omega_{\theta(n+2),\theta}^{(m)} - \frac{3G+\lambda}{2G+\lambda}\Omega_{\theta(n+2),\theta}^{(m)}\right\}$$
$$= \frac{2G}{2G+\lambda}(\lambda_m + n + 1)\Psi_{zn}^{(m)} + \frac{4G}{2G+\lambda}\Omega_{rn}^{(m)}, \quad (29)$$

$$\frac{h^2}{15}\left\{(\lambda_m + n + 3)(\lambda_m + n + 1)\Omega_{\theta(n+2)}^{(m)} + \frac{2G+\lambda}{G}\Omega_{\theta(n+2),\theta\theta}^{(m)}\right.$$
$$\left. + \frac{G+\lambda}{G}(\lambda_m + n + 2)\Omega_{r(n+2),\theta}^{(m)} + \frac{3G+\lambda}{G}\Omega_{r(n+2),\theta}^{(m)}\right\}$$
$$= -\left\{2\Psi_{zn,\theta}^{(m)} + 4\Omega_{\theta n}^{(m)}\right\}, \quad (30)$$

$$(\lambda_m + n + 3)(\lambda_m + n + 1)U_{n+2}^{(m)} + \frac{G}{2G+\lambda}U_{n+2,\theta\theta}^{(m)}$$
$$+ \frac{(G+\lambda)(\lambda_m + n + 2) - (3G+\lambda)}{2G+\lambda}V_{n+2,\theta}^{(m)}$$
$$+ \frac{h^2}{12}\left\{(\lambda_m + n + 3)(\lambda_m + n + 1)\Omega_{r(n+2)}^{(m)}\right.$$
$$+ \frac{G}{2G+\lambda}\Omega_{r(n+2),\theta\theta}^{(m)}$$
$$\left. + \frac{(G+\lambda)(\lambda_m + n + 2) - (3G+\lambda)}{2G+\lambda}\Omega_{\theta(n+2),\theta}^{(m)}\right\}$$
$$= -\frac{\lambda}{2G+\lambda}(\lambda_m + n + 1)\Psi_{zn}^{(m)}, \quad (31)$$

$$(\lambda_m + n + 3)(\lambda_m + n + 1)V_{n+2}^{(m)} + \frac{2G+\lambda}{G}V_{n+2,\theta\theta}^{(m)}$$
$$+ \frac{(G+\lambda)(\lambda_m + n + 2) + (3G+\lambda)}{G}U_{n+2,\theta}^{(m)}$$
$$+ \frac{h^2}{12}\left\{(\lambda_m + n + 3)(\lambda_m + n + 1)\Omega_{\theta(n+2)}^{(m)}\right.$$
$$+ \frac{2G+\lambda}{G}\Omega_{\theta(n+2),\theta\theta}^{(m)}$$
$$\left. + \frac{(G+\lambda)(\lambda_m + n + 2) + (3G+\lambda)}{G}\Omega_{r(n+2),\theta}^{(m)}\right\}$$
$$= -\frac{\lambda}{G}\Psi_{zn,\theta}^{(m)}, \quad (32)$$

$$\frac{\lambda}{G}[(\lambda_m + n + 3)U_{n+2}^{(m)} + V_{n+2,\theta}^{(m)}] - \frac{h^2}{12}\left\{(\lambda_m + n + 3)^2\right.$$
$$\Psi_{z(n+2)}^{(m)} + \Psi_{z(n+2),\theta\theta}^{(m)} + \frac{2G-\lambda}{G}[(\lambda_m + n + 3)\Omega_{r(n+2)}^{(m)}$$
$$\left. + \Omega_{\theta(n+2),\theta}^{(m)}]\right\} = -\frac{2G+\lambda}{G}\Psi_{zn}^{(m)}, \quad (33)$$

and

$$\frac{G}{2G+\lambda}\Omega_{r0,\theta\theta}^{(m)} + (\lambda_m + 1)(\lambda_m - 1)\Omega_{r0}^{(m)}$$
$$+ \frac{(G+\lambda)\lambda_m - (3G+\lambda)}{2G+\lambda}\Omega_{\theta0,\theta}^{(m)} = 0, \quad (34)$$

$$\frac{2G+\lambda}{G}\Omega_{\theta0,\theta\theta}^{(m)} + (\lambda_m + 1)(\lambda_m - 1)\Omega_{\theta0}^{(m)}$$
$$+ \frac{(G+\lambda)\lambda_m + (3G+\lambda)}{G}\Omega_{r0,\theta}^{(m)} = 0, \quad (35)$$

$$\frac{G}{2G+\lambda}U_{0,\theta\theta}^{(m)} + (\lambda_m + 1)(\lambda_m - 1)U_0^{(m)}$$
$$+ \frac{(G+\lambda)\lambda_m - (3G+\lambda)}{2G+\lambda}V_{0,\theta}^{(m)}$$
$$+ \frac{h^2}{12}\left\{\frac{G}{2G+\lambda}\Omega_{r0,\theta\theta}^{(m)} + (\lambda_m + 1)(\lambda_m - 1)\Omega_{r0}^{(m)}\right.$$
$$\left. + \frac{(G+\lambda)\lambda_m - (3G+\lambda)}{2G+\lambda}\Omega_{\theta0,\theta}^{(m)}\right\} = 0, \quad (36)$$

$$\frac{2G+\lambda}{G}V_{0,\theta\theta}^{(m)} + (\lambda_m + 1)(\lambda_m - 1)V_0^{(m)}$$
$$+ \frac{(G+\lambda)\lambda_m + (3G+\lambda)}{G}U_{0,\theta}^{(m)}$$
$$+ \frac{h^2}{12}\left\{\frac{2G+\lambda}{G}\Omega_{\theta0,\theta\theta}^{(m)} + (\lambda_m + 1)(\lambda_m - 1)\Omega_{\theta0}^{(m)}\right.$$
$$\left. + \frac{(G+\lambda)\lambda_m + (3G+\lambda)}{G}\Omega_{r0,\theta}^{(m)}\right\} = 0, \quad (37)$$

$$\frac{\lambda}{G}\left\{(\lambda_m + 1)U_0^{(m)} + V_{0,\theta}^{(m)}\right\} - \frac{h^2}{12}\left\{\Psi_{z0,\theta\theta}^{(m)} + (\lambda_m + 1)^2\Psi_{z0}^{(m)}\right.$$
$$\left. + \frac{2G-\lambda}{G}[\Omega_{\theta0,\theta}^{(m)} + (\lambda_m + 1)\Omega_{r0}^{(m)}]\right\} = 0. \quad (38)$$

Through lengthy and tedious mathematical operations, one can find the general solutions for Eqs. (34)–(38) given as follows:

$$U_0^{(m)} = A_1\cos(\lambda_m + 1)\theta + A_2\sin(\lambda_m + 1)\theta$$
$$+ A_3\cos(\lambda_m - 1)\theta + A_4\sin(\lambda_m - 1)\theta, \quad (39)$$

$$V_0^{(m)} = A_2\cos(\lambda_m + 1)\theta - A_1\sin(\lambda_m + 1)\theta$$
$$+ k_1[A_4\cos(\lambda_m - 1)\theta - A_3\sin(\lambda_m - 1)\theta], \quad (40)$$

$$\Omega_{r0}^{(m)} = C_1\cos(\lambda_m + 1)\theta + C_2\sin(\lambda_m + 1)\theta$$
$$+ C_3\cos(\lambda_m - 1)\theta + C_4\sin(\lambda_m - 1)\theta, \quad (41)$$

$$\Omega_{\theta 0}^{(m)} = C_2 \cos(\lambda_m + 1)\theta - C_1 \sin(\lambda_m + 1)\theta$$
$$+ k_1[C_4 \cos(\lambda_m - 1)\theta - C_3 \sin(\lambda_m - 1)\theta], \qquad (42)$$

$$\Psi_{z0}^{(m)} = E_1 \cos(\lambda_m + 1)\theta + E_2 \sin(\lambda_m + 1)\theta$$
$$+ k_2[A_3 \cos(\lambda_m - 1)\theta + A_4 \sin(\lambda_m - 1)\theta]$$
$$+ k_3[C_3 \cos(\lambda_m - 1)\theta + C_4 \sin(\lambda_m - 1)\theta], \qquad (43)$$

where $k_1 = \frac{3+\lambda_m-4v}{-3+\lambda_m+4v}$, $k_2 = \frac{-24v}{h^2(-3+\lambda_m+4v)}$, $k_3 = \frac{2(1-3v)}{-3+\lambda_m+4v}$, and v is the Poisson's ratio. In Eqs. (39)–(43), the characteristic value λ_m and the coefficients E_1, E_2, A_i, and C_i ($i = 1, 2, 3, 4$) are determined by satisfying the boundary conditions along radial edges.

$U_n^{(m)}$, $V_n^{(m)}$, $\Omega_{rn}^{(m)}$, $\Omega_{\theta n}^{(m)}$, and $\Psi_{zn}^{(m)}$ for $n \geqslant 1$ are determined by solving Eqs. (29)–(33). However, these solutions are not related to the singularities of the stress resultants, so they will not be considered further here.

Notably, one can also start to construct the series solution by assuming the following form of the general solutions for Eqs. (15), (16), (20), (26), and (27):

$$u = \sum_{m=0}^{\infty} \sum_{n=0,2}^{\infty} r^{\lambda_m+n+l_1} U_n^{(m)}(\theta, \lambda_m),$$

$$v = \sum_{m=0}^{\infty} \sum_{n=0,2}^{\infty} r^{\lambda_m+n+l_2} V_n^{(m)}(\theta, \lambda_m),$$

$$\xi_r = \sum_{m=0}^{\infty} \sum_{n=0,2}^{\infty} r^{\lambda_m+n+l_3} \Omega_{rn}^{(m)}(\theta, \lambda_m),$$

$$\xi_\theta = \sum_{m=0}^{\infty} \sum_{n=0,2}^{\infty} r^{\lambda_m+n+l_4} \Omega_{\theta n}^{(m)}(\theta, \lambda_m),$$

$$\psi_z = \sum_{m=0}^{\infty} \sum_{n=0,2}^{\infty} r^{\lambda_m+n+l_5} \Psi_{zn}^{(m)}(\theta, \lambda_m), \qquad (44)$$

where l_i ($i = 1, 2, \ldots, 5$) are either one or zero. Following the above procedure of constructing the solutions, one discovers that the solution form given by Eq. (28) is the only one resulting in the Williams-type singularities of stress resultants.

3.2. Characteristic equations and singularities for stress resultants

As mentioned earlier, the characteristic values, λ_m, are determined by satisfying the boundary conditions

along the radial edges of a corner. Two types of boundary conditions along a radial edge are considered here:

free: $N_\theta, N_{r\theta}, R_\theta, P_\theta,$ and $P_{r\theta} = 0,$ (45a)

clamped: $u, v, \xi_r, \xi_\theta,$ and $\psi_z = 0.$ (45b)

These two cases can be combined to give three distinct problems concerning a wedge.

Substituting Eqs. (39)–(43) and Eq. (28), with $n = 0$, into Eqs. (45a) or (45b) with $\theta = 0$ and α, where α is the vertex angle of the wedge, yields the vanishing determinant of a 10×10 coefficient matrix. Then, the characteristic equations for λ_m can be established. Notably, when the same boundary conditions are imposed along the two radial edges, the symmetry of the problem can be taken advantage of, by considering $-\alpha/2 \leqslant \theta \leqslant \alpha/2$, and separately considering the symmetric and antisymmetric parts of the solution given in Eqs. (39)–(43). For example, considering the symmetric behavior of a wedge with two fixed radial edges, Eqs. (39)–(43), with $A_2 = A_4 = C_2 = C_4 = E_2 = 0$, are substituted into Eq. (45b), the determinant of the resulting 5×5 coefficient matrix is expanded, and

$$\left(\sin \lambda_m \alpha - \frac{\lambda_m}{3 - 4v} \sin \alpha \right) \cos(\lambda_m + 1)\alpha/2 = 0 \qquad (46)$$

is obtained. However, $\cos(\lambda_m + 1)\alpha/2 = 0$ yields $A_1 = A_3 = C_1 = C_3 = 0$ and does not give any stress singularities at the vertex of the wedge. Accordingly, it is discarded. Table 1 lists the characteristic equations for three possible combinations of boundary conditions along the two radial edges. These characteristic equations are not related to the thickness of the plate. Poisson's ratio is the only material property involved in these characteristic equations.

For comparison, Table 1 also summarizes the characteristic equations given by Williams [8] for generalized plane stress in thin plates. The characteristic equations in this work differ from Williams' when the clamped boundary condition is applied, because Lo's plate theory does not use the generalized plane stress condition. Note that if v in the characteristic equations presented herein is replaced by $v/1 + v$, then the resulting characteristic equations are identical to Williams'.

Table 1
Characteristic equations for plates under extension

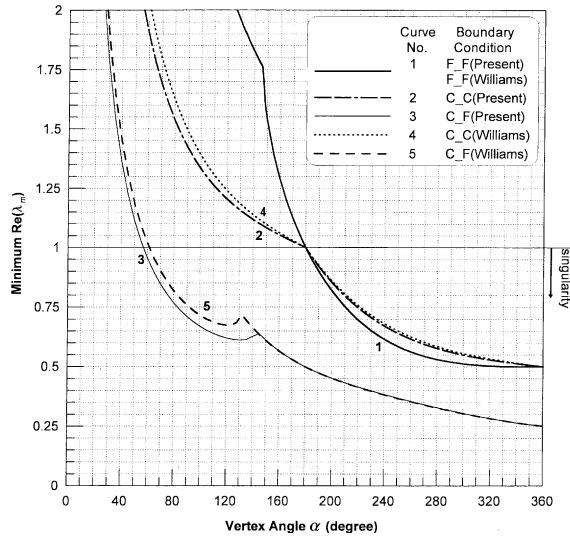| Case no.	Boundary conditions	Present	Thin plate theory [8]
1	Free–free	$\sin \lambda_m \alpha = \pm \lambda_m \sin \alpha$	$\sin \lambda_m \alpha = \pm \lambda_m \sin \alpha$
2	Clamped–clamped	$\sin \lambda_m \alpha = \pm \frac{\lambda_m}{-3+4v} \sin \alpha$	$\sin \lambda_m \alpha = \pm \left(\frac{1+v}{-3+v}\right) \lambda_m \sin \alpha$
3	Clamped–free	$\sin^2 \lambda_m \alpha = \frac{-4(-1+v)^2}{-3+4v} + \frac{\lambda_m^2}{-3+4v} \sin^2 \alpha$	$\sin^2 \lambda_m \alpha = \frac{4}{(3-v)(1+v)} - \left(\frac{1+v}{3-v}\right) \lambda_m^2 \sin^2 \alpha$

Fig. 2. Variation of minimum $\text{Re}(\lambda_m)$ with vertex angle (extension).

Fig. 2 shows the smallest positive real part of λ_m varies with the vertex angle (α) for three combinations of boundary conditions after the roots of the characteristic equations given in Table 1 are numerically determined. The results were computed for $\upsilon = 0.3$. In the legend of Fig. 2, "C" and "F" denote clamped and free boundary conditions, respectively.

Fig. 2 depicts that no singularities exist for N_r, N_θ, N_z, $N_{r\theta}$, P_r, P_θ, and $P_{r\theta}$ when the vertex angle is less than approximately 57°. However, singularities always arise for $\alpha > 180°$, regardless of which of the three combinations of boundary conditions around the vertex is considered. Among the three combinations of boundary conditions considered here, boundary condition C_F provides the strongest singularity. As the vertex angle approaches 2π (i.e., a crack), the singular order of stress resultants at the tip of the crack approaches $r^{-3/4}$ for the boundary condition C_F, while the boundary conditions C_C and F_F yield an order of $r^{-1/2}$. Comparing the present results with Williams' reveals that the orders of stress singularities associated with Lo's plate theory are very close to those according to generalized plane stress theory, except those that involve the boundary condition C_F with approximately $\alpha < 142°$.

4. Stress singularities for plates in bending

Recall that Eqs. (17)–(19) and (23)–(25) are for plates under bending. Through mathematical manipulation of these equations, we can obtain the following equations, which are simpler than Eqs. (17)–(19) and (23)–(25):

$$\frac{2\lambda}{G}\left(\psi_{r,r} + \frac{\psi_r}{r} + \frac{\psi_{\theta,\theta}}{r}\right) + \frac{4(2G+\lambda)}{G}\xi_z$$
$$-\frac{h^2}{15}\left(\xi_{z,rr} + \frac{\xi_{z,r}}{r} + \frac{\xi_{z,\theta\theta}}{r^2}\right)$$
$$+\frac{h^2}{20}\frac{-4G+6\lambda}{G}\left(\phi_{r,r} + \frac{\phi_r}{r} + \frac{\phi_{\theta,\theta}}{r}\right) = 0, \tag{47}$$

$$\frac{8G}{h^2(2G+\lambda)}(w_{,r}+\psi_r) + \frac{2G}{2G+\lambda}\xi_{z,r} + \frac{6G}{2G+\lambda}\phi_r$$
$$-\frac{h^2}{35}\left(\phi_{r,rr} + \frac{\phi_{r,r}}{r} - \frac{\phi_r}{r^2} + \frac{G}{2G+\lambda}\frac{\phi_{r,\theta\theta}}{r^2} + \frac{G+\lambda}{2G+\lambda}\frac{\phi_{\theta,r\theta}}{r}\right.$$
$$\left.-\frac{3G+\lambda}{2G+\lambda}\frac{\phi_{\theta,\theta}}{r^2}\right) = 0, \tag{48}$$

$$\frac{8}{h^2}\left(\frac{w_{,\theta}}{r}+\psi_\theta\right) + \frac{2\xi_{z,\theta}}{r} + 6\phi_\theta - \frac{h^2}{35}\left(\phi_{\theta,rr} + \frac{\phi_{\theta,r}}{r} - \frac{\phi_\theta}{r^2}\right.$$
$$\left.+\frac{2G+\lambda}{G}\frac{\phi_{\theta,\theta\theta}}{r^2} + \frac{G+\lambda}{G}\frac{\phi_{r,r\theta}}{r} + \frac{3G+\lambda}{G}\frac{\phi_{r,\theta}}{r^2}\right) = 0, \tag{49}$$

$$\frac{6}{7h^2}\left(\frac{w_{,\theta}}{r}+\psi_\theta\right) + \left(\frac{19}{70}+\frac{2\lambda}{35G}\right)\frac{\xi_{z,\theta}}{r} + \frac{57}{70}\phi_\theta$$
$$+\frac{1}{35}\left(\phi_{\theta,rr} + \frac{\phi_{\theta,r}}{r} - \frac{\phi_\theta}{r^2} + \frac{2G+\lambda}{G}\frac{\phi_{\theta,\theta\theta}}{r^2} + \frac{G+\lambda}{G}\frac{\phi_{r,r\theta}}{r}\right.$$
$$\left.+\frac{3G+\lambda}{G}\frac{\phi_{r,\theta}}{r^2}\right) = 0, \tag{50}$$

$$\frac{6G}{7h^2(2G+\lambda)}(w_{,r}+\psi_r) + \left(\frac{19G}{70}+\frac{2\lambda}{35}\right)\frac{1}{2G+\lambda}\xi_{z,r}$$
$$+\frac{57G}{70(2G+\lambda)}\phi_r + \frac{1}{35}\left(\phi_{r,rr} + \frac{\phi_{r,r}}{r} - \frac{\phi_r}{r^2} + \frac{G}{2G+\lambda}\frac{\phi_{r,\theta\theta}}{r^2}\right.$$
$$\left.+\frac{G+\lambda}{2G+\lambda}\frac{\phi_{\theta,r\theta}}{r} - \frac{3G+\lambda}{2G+\lambda}\frac{\phi_{\theta,\theta}}{r^2}\right) = 0, \tag{51}$$

$$\frac{1}{15}\left(w_{,rr} + \frac{w_{,r}}{r} + \frac{w_{,\theta\theta}}{r^2}\right) + \left(\frac{1}{15}+\frac{\lambda}{6G}\right)\left(\psi_{r,r} + \frac{\psi_r}{r} + \frac{\psi_{\theta,\theta}}{r}\right)$$
$$+\frac{2G+\lambda}{3G}\xi_z + \frac{h^2\lambda}{40G}\left(\phi_{r,r} + \frac{\phi_r}{r} + \frac{\phi_{\theta,\theta}}{r}\right) = 0. \tag{52}$$

For example, Eq. (47) was obtained by subtracting Eq. (23) from Eq. (17), while Eq. (48) was obtained by subtracting Eq. (24) from Eq. (18).

4.1. Construction of the series solution

To establish the series solution for Eqs. (47)–(52) using the eigenfunction expansion approach, the following solution form is used:

$$w = \sum_{m=0}^{\infty} \sum_{n=0,2}^{\infty} r^{\bar{\lambda}_m+n+1} W_n^{(m)}(\theta, \bar{\lambda}_m),$$

$$\xi_z = \sum_{m=0}^{\infty} \sum_{n=0,2}^{\infty} r^{\bar{\lambda}_m+n+1} \Omega_{zn}^{(m)}(\theta, \bar{\lambda}_m),$$

$$\psi_r = \sum_{m=0}^{\infty} \sum_{n=0,2}^{\infty} r^{\bar{\lambda}_m+n} \Psi_{rn}^{(m)}(\theta, \bar{\lambda}_m),$$

$$\psi_\theta = \sum_{m=0}^{\infty} \sum_{n=0,2}^{\infty} r^{\bar{\lambda}_m+n} \Psi_{\theta n}^{(m)}(\theta, \bar{\lambda}_m), \qquad (53)$$

$$\phi_r = \sum_{m=0}^{\infty} \sum_{n=0,2}^{\infty} r^{\bar{\lambda}_m+n} \Phi_{rn}^{(m)}(\theta, \bar{\lambda}_m),$$

$$\phi_\theta = \sum_{m=0}^{\infty} \sum_{n=0,2}^{\infty} r^{\bar{\lambda}_m+n} \Phi_{\theta n}^{(m)}(\theta, \bar{\lambda}_m),$$

where the characteristic values $\bar{\lambda}_m$ are again assumed to be constants and can be complex numbers. It is also noted that odd n in the above equation will not produce any additional solution, so they are not included.

The real part of $\bar{\lambda}_m$ must exceed zero to satisfy the regularity conditions at the apex of the wedge. Notably, $\bar{\lambda}_m$ with a real part smaller than one leads to singularities of M_r, M_θ, M_z, $M_{r\theta}$, $\overline{M}_r$, $\overline{M}_\theta$ and $\overline{M}_{r\theta}$ at the vertex but no singularities for Q_r, Q_θ, S_r and S_θ, which can be discovered from the relationships between these stress resultants and the displacement functions given in Eqs. (14e)–(14j) and (14p)–(14t).

Substituting Eq. (53) into Eqs. (47)–(52), the vanishing of the coefficients corresponding to the smallest order in r for each equation results in

$$\frac{2\lambda}{G}(\bar{\lambda}_m+1)\Psi_{r0}^{(m)} + \frac{2\lambda}{G}\Psi_{\theta0,\theta}^{(m)} - \frac{h^2}{15}(\Omega_{z0,\theta\theta}^{(m)} + (\bar{\lambda}_m+1)^2\Omega_{z0}^{(m)})$$
$$+ \frac{h^2}{20}\frac{-4G+6\lambda}{G}\left\{(\bar{\lambda}_m+1)\Phi_{r0}^{(m)} + \Phi_{\theta0,\theta}^{(m)}\right\} = 0, \qquad (54)$$

$$\frac{G}{2G+\lambda}\Phi_{r0,\theta\theta}^{(m)} + (\bar{\lambda}_m+1)(\bar{\lambda}_m-1)\Phi_{r0}^{(m)}$$
$$+ \frac{(G+\lambda)\bar{\lambda}_m - (3G+\lambda)}{2G+\lambda}\Phi_{\theta0,\theta}^{(m)} = 0, \qquad (55)$$

$$\frac{2G+\lambda}{G}\Phi_{\theta0,\theta\theta}^{(m)} + (\bar{\lambda}_m+1)(\bar{\lambda}_m-1)\Phi_{\theta0}^{(m)}$$
$$+ \frac{(G+\lambda)\bar{\lambda}_m + (3G+\lambda)}{G}\Phi_{r0,\theta}^{(m)} = 0, \qquad (56)$$

$$\frac{G}{2G+\lambda}\Psi_{r0,\theta\theta}^{(m)} + (\bar{\lambda}_m+1)(\bar{\lambda}_m-1)\Psi_{r0}^{(m)}$$
$$+ \frac{(G+\lambda)\bar{\lambda}_m - (3G+\lambda)}{2G+\lambda}\Psi_{\theta0,\theta}^{(m)} = 0, \qquad (57)$$

$$\frac{2G+\lambda}{G}\Psi_{\theta0,\theta\theta}^{(m)} + (\bar{\lambda}_m+1)(\bar{\lambda}_m-1)\Psi_{\theta0}^{(m)}$$
$$+ \frac{(G+\lambda)\bar{\lambda}_m + (3G+\lambda)}{G}\Psi_{r0,\theta}^{(m)} = 0, \qquad (58)$$

$$\frac{1}{15}\left\{W_{0,\theta\theta}^{(m)} + (\bar{\lambda}_m+1)^2 W_0^{(m)}\right\} + \left(\frac{1}{15}+\frac{\lambda}{6G}\right)\left\{\Psi_{\theta0,\theta}^{(m)}\right.$$
$$+ (\bar{\lambda}_m+1)\Psi_{r0}^{(m)}\right\} + \frac{h^2\lambda}{40G}\left\{\Phi_{\theta0,\theta}^{(m)} + (\bar{\lambda}_m+1)\Phi_{r0}^{(m)}\right\} = 0. \qquad (59)$$

The general homogeneous solutions for the above differential equations are

$$W_0^{(m)} = \widetilde{A}_1 \cos(\bar{\lambda}_m+1)\theta + \widetilde{A}_2 \sin(\bar{\lambda}_m+1)\theta$$
$$+ k_6[\widetilde{B}_3 \cos(\bar{\lambda}_m-1)\theta + \widetilde{B}_4 \sin(\bar{\lambda}_m-1)\theta]$$
$$+ k_7[\widetilde{E}_3 \cos(\bar{\lambda}_m-1)\theta + \widetilde{E}_4 \sin(\bar{\lambda}_m-1)\theta], \qquad (60)$$

$$\Psi_{r0}^{(m)} = \widetilde{B}_1 \cos(\bar{\lambda}_m+1)\theta + \widetilde{B}_2 \sin(\bar{\lambda}_m+1)\theta$$
$$+ \widetilde{B}_3 \cos(\bar{\lambda}_m-1)\theta + \widetilde{B}_4 \sin(\bar{\lambda}_m-1)\theta, \qquad (61)$$

$$\Psi_{\theta0}^{(m)} = \widetilde{B}_2 \cos(\bar{\lambda}_m+1)\theta - \widetilde{B}_1 \sin(\bar{\lambda}_m+1)\theta$$
$$+ k_1[\widetilde{B}_4 \cos(\bar{\lambda}_m-1)\theta - \widetilde{B}_3 \sin(\bar{\lambda}_m-1)\theta], \qquad (62)$$

$$\Phi_{r0}^{(m)} = \widetilde{E}_1 \cos(\bar{\lambda}_m+1)\theta + \widetilde{E}_2 \sin(\bar{\lambda}_m+1)\theta$$
$$+ \widetilde{E}_3 \cos(\bar{\lambda}_m-1)\theta + \widetilde{E}_4 \sin(\bar{\lambda}_m-1)\theta, \qquad (63)$$

$$\Phi_{\theta0}^{(m)} = \widetilde{E}_2 \cos(\bar{\lambda}_m+1)\theta - \widetilde{E}_1 \sin(\bar{\lambda}_m+1)\theta$$
$$+ k_1[\widetilde{E}_4 \cos(\bar{\lambda}_m-1)\theta - \widetilde{E}_3 \sin(\bar{\lambda}_m-1)\theta], \qquad (64)$$

$$\Omega_{z0}^{(m)} = \widetilde{D}_1 \cos(\bar{\lambda}_m+1)\theta + \widetilde{D}_2 \sin(\bar{\lambda}_m+1)\theta$$
$$+ k_4[\widetilde{B}_3 \cos(\bar{\lambda}_m-1)\theta + \widetilde{B}_4 \sin(\bar{\lambda}_m-1)\theta]$$
$$+ k_5[\widetilde{E}_3 \cos(\bar{\lambda}_m-1)\theta + \widetilde{E}_4 \sin(\bar{\lambda}_m-1)\theta], \qquad (65)$$

where $k_4 = -\frac{60v}{h^2(-3+\bar{\lambda}_m+4v)}$, $k_5 = \frac{3(1-5v)}{-3+\bar{\lambda}_m+4v}$, $k_6 = \frac{1+3v}{-3+\bar{\lambda}_m+4v}$, and $k_7 = \frac{3vh^2}{4(-3+\bar{\lambda}_m+4v)}$. The characteristic value $\bar{\lambda}_m$ and the coefficients $\widetilde{A}_1$, $\widetilde{A}_2$, $\widetilde{D}_1$, $\widetilde{D}_2$, $\widetilde{B}_i$, and $\widetilde{E}_i$ $(i = 1, 2, 3, 4)$ are determined from the boundary conditions along the two radial edges of the wedge.

4.2. Characteristic equations

Four types of homogeneous boundary conditions along a radial edge are considered here to elucidate the stress singularities at the vertex of the wedge:

clamped: $\quad w = \psi_r = \psi_\theta = \phi_r = \phi_\theta = \xi_z = 0$, (66a)

free: $\quad Q_\theta = M_{r\theta} = M_\theta = \overline{M}_{r\theta} = \overline{M}_\theta = S_\theta = 0$, (66b)

type I simply supported: $\quad w = \psi_r = \phi_r = \xi_z$
$$= M_\theta = \overline{M}_\theta = 0, \qquad (66c)$$

type II simply supported: $\quad w = M_{r\theta} = M_\theta$
$$= \overline{M}_{r\theta} = \overline{M}_\theta = S_\theta = 0. \qquad (66d)$$

For simplicity, in the following, the clamped and free boundary conditions are denoted by C and F, respectively, while type I and type II simply supported boundary conditions are represented by S(I) and S(II), respectively.

Substituting Eqs. (60)–(65) and Eq. (53) with $n = 0$ into the prescribed boundary conditions along two radial edges yields twelve linear homogeneous algebraic equations in $\tilde{A}_1$, $\tilde{A}_2$, $\tilde{D}_1$, $\tilde{D}_2$, $\tilde{B}_i$, and $\tilde{E}_i$ ($i = 1, 2, 3, 4$). The vanishing determinant of the 12×12 coefficient matrix from the twelve equations yields the characteristic equations for $\bar{\lambda}_m$.

Table 2 lists the characteristic equations for 10 combinations of the boundary conditions. These characteristic equations are again not related to the thickness of the plate. Again, Poisson's ratio is the only material property involved in these characteristic equations. Some boundary conditions yield the same characteristic equations. The boundary conditions F_F, S(II)_S(II), and S(II)_F lead to the same characteristic equation, while the boundary conditions S(I)_F and S(I)_S(II) also share the same characteristic equation. The C_F boundary condition gives the same characteristic equation as does
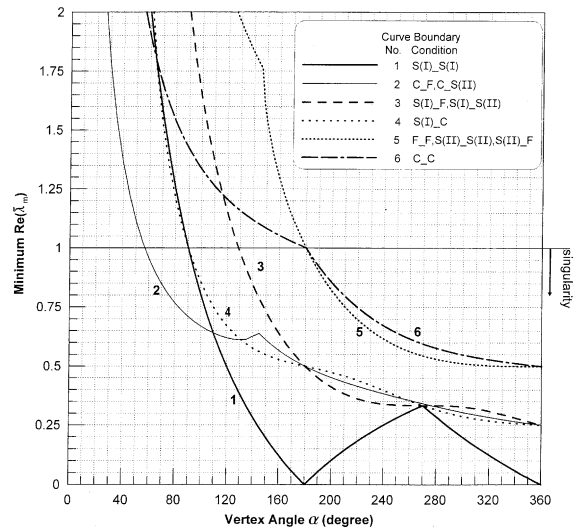

Fig. 3. Variation of minimum $\text{Re}(\bar{\lambda}_m)$ with vertex angle (bending).

Table 2
Characteristic equations for plates under bending

Case no.	Boundary conditions	Present	Reddy's refined plate theory [23]
1	Simply supported (I)–simply supported (I)	$\cos \bar{\lambda}_m \alpha = \pm \cos \alpha$	$\cos \bar{\lambda} \alpha = \pm \cos \alpha$ [a,b]
2	Clamped–free	$\sin^2 \bar{\lambda}_m \alpha = \frac{-4(-1+v)^2}{-3+4v} + \frac{\bar{\lambda}_m^2}{-3+4v} \sin^2 \alpha$	$\sin^2 \bar{\lambda}_m \alpha = \frac{4 - \bar{\lambda}_m^2 (1+v)^2 \sin^2 \alpha}{(3-v)(1+v)}$ [a] $\sin^2 \bar{\lambda}_m \alpha = \frac{4 - \bar{\lambda}_m^2 (1-v)^2 \sin^2 \alpha}{(3+v)(1-v)}$ [b]
3	Simply supported (I)–free	$\sin 2\bar{\lambda}_m \alpha = \bar{\lambda}_m \sin 2\alpha$	$\sin 2\bar{\lambda}_m \alpha = \bar{\lambda}_m \sin 2\alpha$ [a] $\sin 2\bar{\lambda}_m \alpha = \frac{\lambda_m (1-v)}{-3-v} \sin 2\alpha$ [b]
4	Simply supported (I)–clamped	$\sin 2\bar{\lambda}_m \alpha = \frac{\bar{\lambda}_m}{-3+4v} \sin 2\alpha$	$\sin 2\bar{\lambda}_m \alpha = \frac{\lambda_m (1+v)}{-3+v} \sin 2\alpha$ [a] $\sin 2\bar{\lambda}_m \alpha = \bar{\lambda}_m \sin 2\alpha$ [b]
5	Free–free	$\sin \bar{\lambda}_m \alpha = \pm \bar{\lambda}_m \sin \alpha$	$\sin \bar{\lambda}_m \alpha = \pm \bar{\lambda}_m \sin \alpha$ [a] $\sin \bar{\lambda}_m \alpha = \pm \frac{\bar{\lambda}_m (1-v)}{-3-v} \sin \alpha$ [b]
6	Clamped–clamped	$\sin \bar{\lambda}_m \alpha = \pm \frac{\bar{\lambda}_m}{-3+4v} \sin \alpha$	$\sin \bar{\lambda}_m \alpha = \pm \frac{\bar{\lambda}_m (1+v)}{-3+v} \sin \alpha$ [a] $\sin \bar{\lambda}_m \alpha = \pm \bar{\lambda}_m \sin \alpha$ [b]
7	Simply supported (II)–simply supported (II)	$\sin \bar{\lambda}_m \alpha = \pm \bar{\lambda}_m \sin \alpha$	$\sin \bar{\lambda}_m \alpha = \pm \bar{\lambda}_m \sin \alpha$ [a] $\cos \bar{\lambda}_m \alpha = \pm \cos \alpha$
8	Clamped–simply supported (II)	$\sin^2 \bar{\lambda}_m \alpha = \frac{-4(-1+v)^2}{-3+4v} + \frac{\bar{\lambda}_m^2}{-3+4v} \sin^2 \alpha$	$\sin^2 \bar{\lambda}_m \alpha = \frac{4 - \bar{\lambda}_m^2 (1+v)^2 \sin^2 \alpha}{(3-v)(1+v)}$ [a] $\sin 2\bar{\lambda}_m \alpha = \bar{\lambda}_m \sin 2\alpha$
9	Simply supported (I)–simply supported (II)	$\sin 2\bar{\lambda}_m \alpha = \bar{\lambda}_m \sin 2\alpha$	$\sin 2\bar{\lambda}_m \alpha = \bar{\lambda}_m \sin 2\alpha$ [a] $\cos 2\bar{\lambda}_m \alpha = \cos 2\alpha$
10	Simply supported (II)–free	$\sin \bar{\lambda}_m \alpha = \pm \bar{\lambda}_m \sin \alpha$	$\sin \bar{\lambda}_m \alpha = \pm \bar{\lambda}_m \sin \alpha$ [a] $\sin 2\bar{\lambda}_m \alpha = \frac{\bar{\lambda}_m (-1+v)}{3+v} \sin 2\alpha$

Note: "a" means that the equation can be recovered in FSDPT.
"b" means that the equation can be regained in CPT.

the C_S(II) boundary condition. Moreover, the characteristic equations for the bending and extension cases are the same for the boundary conditions C_F and C_C.

For comparison, Table 2 also summarizes the characteristic equations corresponding to various boundary conditions based on CPT [13], FSDPT [20,22] and Reddy's plate theory [23]. Notably, the characteristic equations of Reddy's plate theory include those of CPT and FSDPT, except for those related to the S(II) boundary condition, which does not apply in CPT. Comparing the characteristic equations in Table 2 indicates that different plate theories usually yield different characteristic equations. Interestingly, the char-

acteristic equations obtained herein are exactly the same as those for FSDPT when the clamped boundary condition is not imposed along the radial edges. The boundary condition S(I)_S(I) results in the same characteristic equation for different plate theories.

4.3. Singularities of stress resultants

Fig. 3 displays the minimum positive real part of the characteristic value $\bar{\lambda}_m$, which varies with the vertex angle of the wedge, α, and the boundary conditions. The results were determined for $v = 0.3$. Recall that $\bar{\lambda}_m$ with a real part less than one, leads to the singularities of M_r,
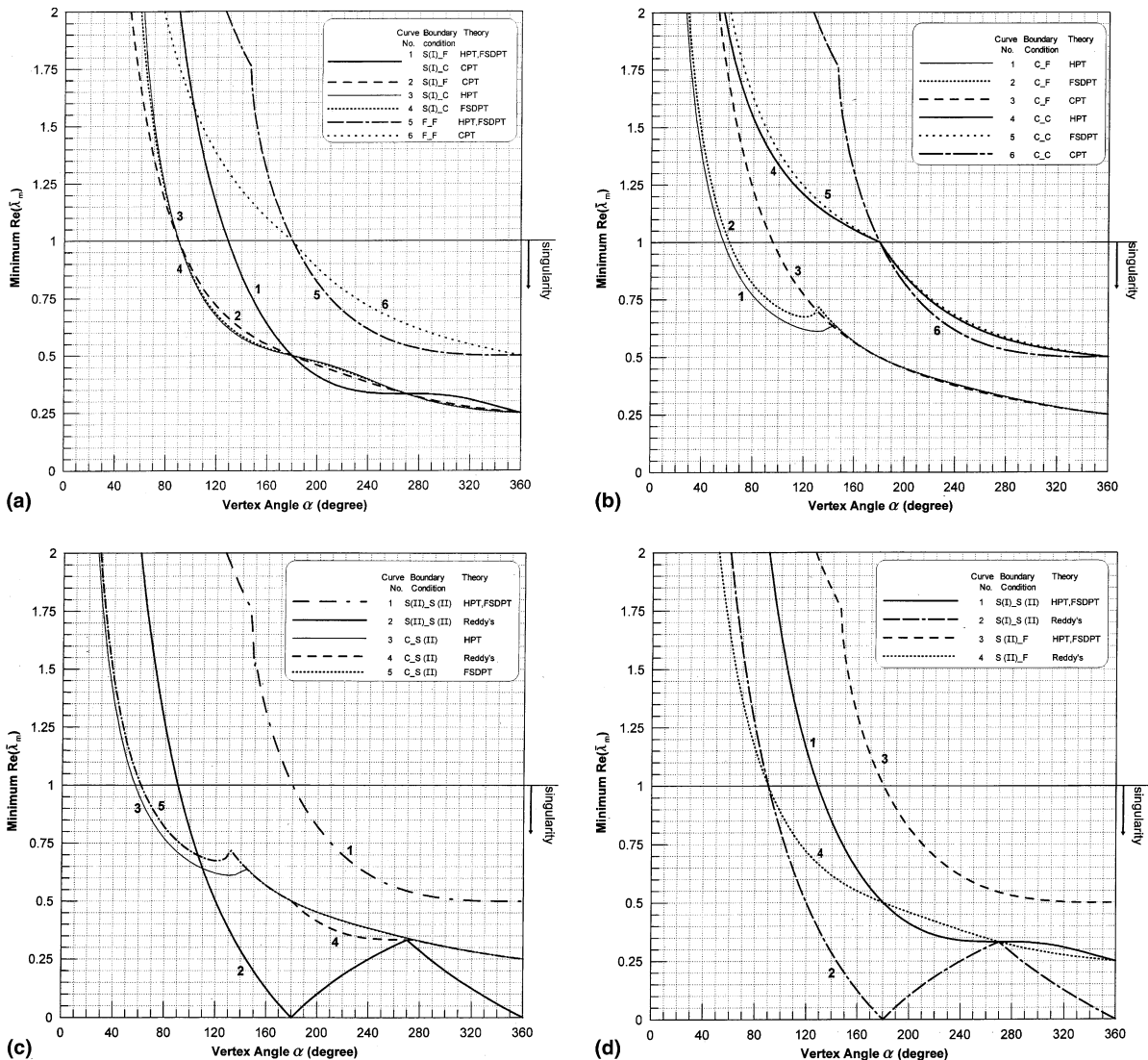

Fig. 4. Comparison of minimum $\mathrm{Re}(\bar{\lambda}_m)$ for different plate theories: (a) for boundary conditions S(I)_F, S(I)_C and F_F, (b) for boundary conditions C_F and C_C, (c) for boundary conditions S(II)_S(II) and C_S(II) and (d) for boundary conditions S(I)_S(II) and S(II)_F.

M_θ, M_z, $M_{r\theta}$, $\overline{M}_r$, $\overline{M}_\theta$ and $\overline{M}_{r\theta}$ at the vertex. No singularities arise for approximately $\alpha < 57°$, while singularities always exist for $\alpha > 180°$. The boundary conditions C_F and C_S(II) produce the strongest singularities at $57° < \alpha < 109°$, while the S(I)_S(I) boundary condition leads to the strongest singularities for $\alpha \geqslant 109°$. The boundary condition C_C yields the weakest singularities among the considered boundary conditions.

Fig. 4a–d compare the minimum positive $\mathrm{Re}(\bar{\lambda}_m)$ obtained using different plate theories. Again, the results were computed for $\upsilon = 0.3$. Recall that the characteristic equations based on Reddy's plate theory consist of those of CPT and FSDPT except for those related to the S(II) boundary condition. Hence, the smallest positive $\mathrm{Re}(\bar{\lambda}_m)$ for Reddy's plate theory in Fig. 4a and b is the smaller of the characteristic values for CPT and FSDPT. The boundary condition S(II) does not occur in CPT, so Fig. 4c and d do not display the results for CPT.

The results in Fig. 4a reveal several important findings. Under the boundary condition S(I)_F, CPT and Reddy's theory produce stronger singularities than does FSDPT or Lo's high-order plate theory (referred to as HPT in the legend) for $90° < \alpha < 180°$ and $270° < \alpha < 360°$. Lo's theory generates the strongest singularities for $90° < \alpha < 180°$ and $270° < \alpha < 360°$ in the case of the S(I)_C boundary condition. However, HPT and FSDPT generate very similar minimum positive $\mathrm{Re}(\bar{\lambda}_m)$ for the boundary condition S(I)_C. For a wedge with two free radial edges, CPT produces weaker singularities at the vertex than does FSDPT, Reddy's theory or HPT.

Fig. 4b indicates that under the C_F boundary condition, HPT yields a smaller positive $\mathrm{Re}(\bar{\lambda}_m)$ than the other theories when α is below about $142°$, while all the theories generate almost identical orders of stress singularities at other angles. More severe singularities occur with CPT and Reddy's theory than with FSDPT and HPT for the C_C boundary condition. Nevertheless, all the theories share the same orders of stress singularities when the vertex angle approaches 2π.

Fig. 4c and d present the minimum positive $\mathrm{Re}(\bar{\lambda}_m)$ for boundary conditions involving S(II). Fig. 4c displays that the minimum positive $\mathrm{Re}(\bar{\lambda}_m)$ for Reddy's theory differs greatly from that for FSDPT and HPT under the S(II)_S(II) boundary condition. The former produces much stronger singularities than the latter. For the C_S(II) boundary condition, Reddy's theory and FSDPT generate identical minimum positive $\mathrm{Re}(\bar{\lambda}_m)$ except for $180° < \alpha < 270°$. For the C_S(II) boundary condition, HPT produces stronger singularities than do FSDPT and Reddy's theory for α below roughly $142°$, while HPT and FSDPT produce almost identical minimum positive $\mathrm{Re}(\bar{\lambda}_m)$ for other angles. Fig. 4d shows that Reddy's theory produces more severe singularities at the vertex than do FSDPT and HPT for the boundary conditions S(I)_S(II) and S(II)_F. Notably, when the vertex angle approaches 2π, the orders of stress singu-

larities obtained using Reddy's theory are different from those obtained using FSDPT and HPT in the cases of the S(II)_S(II), S(II)_F, and S(I)_S(II) boundary conditions, while all the theories share the identical orders of stress singularities for the other boundary conditions.

5. Concluding remarks

This work presented an eigenfunction expansion approach to investigating corner singularities of stress resultants in thick plates based on Lo's high-order plate theory. The singular behaviors of stresses at a sharp corner of a plate under extension and bending were thoroughly studied. The characteristic equations for determining the orders of stress singularities were derived for various combinations of boundary conditions around the vertex of a wedge. The thickness of the plate does not affect the orders of stress singularities, while Poisson's ratio is the only material property that can possibly influence the singularity behavior.

For a wedge under extension, Lo's high-order plate theory and the theory that uses the generalized plane stress assumption yield the same characteristic equation for the F_F boundary condition along the radial edges of the wedge, but they give different characteristic equations for the cases of the C_F and C_C boundary conditions. This difference may follow from the high-order plate theory's using the three-dimensional Hooke's law for stress-strain relations. Nevertheless, these different characteristic equations for the C_C boundary condition produce very similar orders of stress singularities when the Poisson's ratio is 0.3, and generate almost identical singular orders for the C_F boundary condition when the vertex angle exceeds roughly $142°$.

For a plate (wedge) under bending, Lo's high-order plate theory gives the same characteristic equations as FDSPT when the boundary conditions along the radial edges do not involve clamping. Generally, different plate theories, such as CPT, FSDPT, Reddy's refined plate theory, and Lo's high-order plate theory, yield different characteristic equations. However, these plate theories yields identical characteristic equations for the S(I)_S(I) boundary condition. For a plate with a Poisson's ratio of 0.3, Lo's theory does not generate stress singularities when the vertex angle is below $57°$, while a singularity always arises when the vertex angle exceeds π. Moreover, the boundary conditions C_F and C_S(II) produce the strongest singularities for $57° < \alpha < 109°$, while the S(I)_S(I) boundary condition leads to the strongest singularities for $\alpha \geqslant 109°$. Finally, it should be specially noted that Lo's theory does not produce the kind of shear force singularity generated by CPT and FSDPT.

The characteristic equations and the numerical results shown here are very important for dealing with thick plates having sharp corners when Lo's theory is

applied. The stress singularities at the corners have to be appropriately taken into account to obtain accurate solution when such numerical techniques as the finite element method, the finite difference approach, and the Ritz method are used to solve complex plate problems with sharp corners. Notably, Lo's theory may also produce logarithmic stress singularities, and therefore requires further research.

References

[1] Hanna NF. Thick plate theories with applications to vibration. PhD dissertation, Ohio State University, Columbus, OH; 1990.

[2] Stenger F. Numerical methods based on sinc and analytic functions. New York: Springer-Verlag; 1993.

[3] Leissa AW. Singularity considerations in membrane, plate and shell behaviors. Int J Solids Struct 2001;38:3341–53.

[4] Leissa AW, McGee OG, Huang CS. Vibrations of sectorial plates having corner stress singularities. ASME J Appl Mech 1993;60(1):134–40.

[5] Leissa AW, McGee OG, Huang CS. Vibrations of circular plates having V-notches or sharp radial cracks. J Sound Vib 1993;161(2):227–39.

[6] Yosibash Z, Schiff B. A superelement for two-dimensional singular boundary value problems in linear elasticity. Int J Fract 1993;62:325–40.

[7] Abdel Wahab MM, de Roeck G. A 2-D four-noded finite element containing a singularity of order λ. Struct Eng Mech 1995;3(4):383–90.

[8] Williams ML. Stress singularities resulting from various boundary conditions in angular corners of plates in extension. ASME J Appl Mech 1952;19(4):526–8.

[9] Hartranft RJ, Sih GC. The use of eigenfunction expansions in the general solution of three-dimensional crack problems. J Math Mech 1969;19(2):123–38.

[10] Hein VL, Erdogan F. Stress singularities in a two-material wedge. Int J Fract Mech 1971;7(3):317–30.

[11] Ting TCT, Chou SC. Edge singularities in anisotropic composites. Int J Solids Struct 1981;17(11):1057–68.

[12] Xie M, Chaudhuri RA. Three-dimensional stress singularity at a bimaterial interface crack front. Compos Struct 1998;40(2):137–47.

[13] Williams ML. Stress singularities resulting from various boundary conditions in angular corners of plates under bending. Proc 1st US Natl Congress Appl Mech 1952:325–9.

[14] Williams ML, Owens RH. Stress singularities in angular corners of plates having linear flexural rigidities for various boundary conditions. Proc 2nd US Natl Congress Appl Mech 1954:407–11.

[15] Williams ML, Chapkis RL. Stress singularities for a sharp-notched polarly orthotropic plate. Proc 3rd US Natl Congress Appl Mech 1958:281–6.

[16] Rao AK. Stress concentrations and singularities at interfaces corners. Z Angew Math Mech 1971;51:395–406.

[17] Huang CS, Leissa AW, McGee OG. Exact analytical solutions for the vibrations of sectorial plates with simply supported radial edges. ASME J Appl Mech 1993;60:478–83.

[18] Sinclair GB. Logarithmic stress singularities resulting from various boundary conditions in angular corners of plates under bending. ASME J Appl Mech 2000;67:219–23.

[19] Ojikutu IO, Low RO, Scott RA. Stress singularities in laminated composite wedge. Int J Solids Struct 1984;20(8):777–90.

[20] Burton WS, Sinclair GB. On the singularities in Reissner's theory for the bending of elastic plates. ASME J Appl Mech 1986;53:220–2.

[21] Huang CS, McGee OG, Leissa AW. Exact analytical solutions for the vibrations of Mindlin sectorial plates with simply supported radial edges. Int J Solid Struct 1994;31(11):1609–31.

[22] Huang CS. Stress singularities at angular corners in first-order shear deformation plate theory. Int J Mech Sci 2003;45:1–20.

[23] Huang CS. On the singularity induced by boundary conditions in a third-order thick plate theory. ASME J Appl Mech 2002;69:800–10.

[24] Reddy JN. Energy and variational methods in applied mechanics. New York: John Wiley; 1984.

[25] Schmidt R. A refined nonlinear theory for plates with transverse shear deformation. J Ind Math Soc 1977;27(1):23–38.

[26] Krishna Murty AV. Higher order theory for vibration of thick plates. AIAA J 1977;15(2):1823–4.

[27] Bert CW. A critical evaluation of new plate theories applied to composite plates. Compos Struct 1984;2:329–47.

[28] Lo KH, Christensen RM, Wu EM. A high-order theory of plate deformation, part I: homogeneous plates. ASME J Appl Mech 1977;44:669–76.

[29] Doong JL. Vibration and stability of an initially stressed thick plate according to a high-order deformation theory. J Sound Vib 1987;113(3):425–40.

[30] Chen LW, Hwang JR. Vibrations of initially stressed thick circular and annular plates based on a high-order plate theory. J Sound Vib 1988;122(1):79–95.

[31] Chen LW, Hwang JR, Doong JL. Asymmetric dynamic stability of thick annular plates based on a high-order plate theory. J Sound Vib 1989;130(3):425–37.